PROBLEMS IN NONLINEAR ACOUSTICS:

RAYLEIGH WAVES, PULSED SOUND BEAMS, AND WAVEGUIDES

Mark F. Hamilton

DEPARTMENT OF MECHANICAL ENGINEERING
THE UNIVERSITY OF TEXAS AT AUSTIN
AUSTIN, TEXAS 78712-1063

31 August 1993

Fifth Annual Summary Report
ONR Grant N00014-89-J-1003

Prepared for:

OFFICE OF NAVAL RESEARCH
DEPARTMENT OF THE NAVY
ARLINGTON, VA 22217-5000

REPORT DOCUMENTATION PAGE

Form Approved
OMB No. 0704-0188

1. AGENCY USE ONLY *(Leave blank)*	2. REPORT DATE	3. REPORT TYPE AND DATES COVERED
	31 August 1993	Summary 15 Aug 92 - 31 Aug 93

4. TITLE AND SUBTITLE

Problems in Nonlinear Acoustics

5. FUNDING NUMBERS

N00014-89-J-1003

6. AUTHOR(S)

Mark F. Hamilton

7. PERFORMING ORGANIZATION NAME(S) AND ADDRESS(ES)

University of Texas at Austin
Department of Mechanical Engineering
Austin, TX 78712-1063

8. PERFORMING ORGANIZATION REPORT NUMBER

9. SPONSORING/MONITORING AGENCY NAME(S) AND ADDRESS(ES)

Office of Naval Research
Physics Division ONR 312
800 North Quincy Street
Arlington, VA 22217-5660

10. SPONSORING/MONITORING AGENCY REPORT NUMBER

11. SUPPLEMENTARY NOTES

12a. DISTRIBUTION/AVAILABILITY STATEMENT

Approved for public release:
Distribution unlimited.

12b. DISTRIBUTION CODE

13. ABSTRACT *(Maximum 200 words)*

Three project topics, all in the area of nonlinear acoustics, are discussed in this annual summary report: (1) Nonlinear Rayleigh Waves (including diffraction effects in Rayleigh wave beams, local and nonlocal nonlinearity in Rayleigh waves, pulsed nonlinear Rayleigh waves, and nonlinear Stoneley waves); (2) Pulsed Finite Amplitude Sound Beams (including a uniformly valid axial solution for self-demodulation, and measurements of pulsed sound beams in water); and (3) Finite Amplitude Sound in Waveguides.

14. SUBJECT TERMS

nonlinear acoustics, Rayleigh waves, Stoneley waves, diffraction, pulses, self-demodulation, waveguides

15. NUMBER OF PAGES

25

16. PRICE CODE

17. SECURITY CLASSIFICATION OF REPORT	18. SECURITY CLASSIFICATION OF THIS PAGE	19. SECURITY CLASSIFICATION OF ABSTRACT	20. LIMITATION OF ABSTRACT
UNCLASSIFIED	UNCLASSIFIED	UNCLASSIFIED	

CONTENTS

INTRODUCTION

This annual summary report describes research performed from 14 August 1992 through 31 August 1993 with support from ONR under grant N00014-89-J-1003. Three main projects are discussed in this report:

I. Nonlinear Rayleigh Waves

II. Pulsed Finite Amplitude Sound Beams

III. Finite Amplitude Sound in Waveguides

Contributions to these projects were made by the following individuals:

Senior Personnel

- M. F. Hamilton, principal investigator
- Yu. A. Il'insky, visiting scientist
- E. A. Zabolotskaya, visiting scientist

Graduate Students

- M. A. Averkiou, Ph.D. student in Mechanical Engineering
- E. Yu. Knight, M.A. student in Physics
- Y.-S. Lee, Ph.D. student in Mechanical Engineering
- G. D. Meegan, Ph.D. student in Physics
- D. J. Shull, M.S. student in Electrical Engineering
- T. W. VanDoren, Ph.D. student in Mechanical Engineering

Although Professor Il'insky was in Moscow during the entire period covered by this report, he was instrumental in the research performed on nonlinear Rayleigh waves as a result of his visit to Austin during the 1991-92 academic year. Professor Il'insky was consulted frequently by our group during the past academic year. Dr. Zabolotskaya is on leave from the General Physics Institute in Moscow.

The main source of financial support, in addition to that provided by ONR, has been the David and Lucile Packard Foundation Fellowship for Science and Engineering. Computing resources were provided by The University of Texas System Center for High Performance Computing.

The following manuscripts and abstracts, which describe work supported at least in part by ONR, have been published (or submitted for publication) since 14 August 1992.

Refereed Journals

- Yu. A. Il'inskii and E. A. Zabolotskaya, "Cooperative radiation and scattering of acoustic waves by gas bubbles in liquids," *J. Acoust. Soc. Am.* **92**, 2837–2841 (1992).
- M. F. Hamilton, "Transient axial solution for the reflection of a spherical wave from a concave ellipsoidal mirror," *J. Acoust. Soc. Am.* **93**, 1256–1266 (1993).
- C. M. Darvennes and M. F. Hamilton, "Additional remarks on parametric reception near a reflecting plane," *J. Acoust. Soc. Am.* **93**, 3507–3510 (1993).
- M. F. Hamilton, Yu. A. Il'insky, and E. A. Zabolotskaya, "On the existence of stationary nonlinear Rayleigh waves," *J. Acoust. Soc. Am.* **93**, 3089–3095 (1993).
- D. J. Shull, M. F. Hamilton, Yu. A. Il'insky, and E. A. Zabolotskaya, "Harmonic generation in plane and cylindrical nonlinear Rayleigh waves," *J. Acoust. Soc. Am.* **94**, 418–427 (1993).
- M. A. Averkiou, Y.–S. Lee, and M. F. Hamilton, "Self-demodulation of amplitude and frequency modulated pulses in a thermoviscous fluid," *J. Acoust. Soc. Am.* (in press).

Conference Proceedings

- M. F. Hamilton, "A transient solution for the axial pressure field of a spark-source lithotripter," *Proceedings of the 14th International Congress on Acoustics*, edited by P. Li (Beijing, China, 1992), Vol. 1, Paper A5-1.
- M. A. Averkiou, Y.-S. Lee, and M. F. Hamilton, "Self-demodulation revisited," *Advances in Nonlinear Acoustics*, edited by H. Hobæk (World Scientific, Singapore, 1993), pp. 251–256.
- D. J. Shull, M. F. Hamilton, and E. A. Zabolotskaya, "Nonlinear Rayleigh wave beams," *Advances in Nonlinear Acoustics*, edited by H. Hobæk (World Scientific, Singapore, 1993), pp. 496–501.

Oral Presentation Abstracts

- D. J. Shull, M. F. Hamilton, Yu. A. Il'insky, and E. A. Zabolotskaya, "Harmonic interactions in plane and cylindrical nonlinear Rayleigh waves," *J. Acoust. Soc. Am.* **92**, 2358 (1992).
- M. F. Hamilton, Yu. A. Il'insky, and E. A. Zabolotskaya, "On the existence of stationary nonlinear Rayleigh waves," *J. Acoust. Soc. Am.* **92**, 2358 (1992).

- M. F. Hamilton, Yu. A. Il'insky, and E. A. Zabolotskaya, "Rayleigh wave nonlinearity," *J. Acoust. Soc. Am.* **93**, 2384 (1993).

Theses

- C. E. Bruch, "Second harmonic generation in Pekeris waveguides," M.A. Thesis, The University of Texas at Austin (December 1992).
- D. J. Shull, "Harmonic generation in plane, cylindrical, and diffracting nonlinear Rayleigh waves," M.S. Thesis, The University of Texas at Austin (May 1993).
- T. W. VanDoren, "Propagation of finite amplitude sound in multiple waveguide modes," Ph.D. Dissertation, The University of Texas at Austin (August 1993).

I. Nonlinear Rayleigh Waves

Portions of the work described in this section were performed by Yu. A. Il'insky, E. Yu. Knight, G. D. Meegan, D. J. Shull, and E. A. Zabolotskaya. Three projects are described below: diffracting nonlinear Rayleigh wave beams, pulsed nonlinear Rayleigh waves, and local and nonlocal nonlinearity in Rayleigh waves. All three projects are based on the theoretical model developed by Zabolotskaya[1] for the propagation of nonlinear Rayleigh waves in isotropic solids.

A. Diffracting Nonlinear Rayleigh Wave Beams

This project is completed, and it was reported first in Shull's masters thesis.[2] Shull graduated with a masters degree in Electrical Engineering in May 1993. The following discussion is mainly excerpted from the proceedings[3] that accompanied the presentation of this material at the 13th International Symposium on Nonlinear Acoustics (Bergen, Norway, June–July 1993). An article is currently in preparation for submission to *Journal of the Acoustical Society of America*.

Linear theory for diffracting, monofrequency, Rayleigh wave beams is well established.[4] Here, nonlinear effects that produce harmonic generation and waveform distortion in diffracting Rayleigh wave beams are taken into account. The isotropic elastic half space that supports the Rayleigh wave occupies the region $z \leq 0$. The source is in the plane $x = 0$ and it radiates in the $+x$ direction. Of interest here is the effect of finite source width in the y direction, which leads to diffraction in the (x, y) plane.

For simplicity, all equations presented below are in dimensionless form. A complete list of definitions for all parameters needed to perform the calculations may be found elsewhere.[2,5] Only parameters that are necessary for interpretation of the results are provided.

The analysis applies to the horizontal (v_x) and vertical (v_z) components of the particle velocity vector. The components are written in the dimensionless forms $V_x = v_x/v_{0x}$ and $V_z = v_z/v_{0z}$, where v_{0x} and v_{0z} are characteristic source velocity amplitudes, and the following Fourier series expansions are introduced:

$$V_x = \frac{1}{2}\sum_{n=-\infty}^{\infty} V_n(X,Y)U_{xn}(Z)e^{-in\tau} \qquad V_z = \frac{1}{2}\sum_{n=-\infty}^{\infty} V_n(X,Y)U_{zn}(Z)e^{-in\tau} \quad (1)$$

where $X = x/x_0$ is an axial coordinate in terms of the Rayleigh distance $x_0 = k_0a^2/2$, $k_0 = \omega_0/c_R$ is a wavenumber in terms of the fundamental angular frequency ω_0 of the source and the small signal Rayleigh wave speed c_R, a is a characteristic source dimension, $Y = y/a$ is a dimensionless transverse coordinate, $Z = k_0z$ is a dimensionless depth coordinate, and $\tau = \omega_0(t - x/c_R)$ is a retarded time. The functions U_{xn} and U_{zn} describe the depth dependencies, according to linear theory, for the individual harmonic components. The following set of coupled equations can then be derived, within the parabolic approximation, for the finite amplitude behavior of the spectral components in a diffracting beam:[6]

$$\frac{\partial V_n}{\partial X} + \frac{1}{4in}\frac{\partial^2 V_n}{\partial Y^2} + A_nV_n = -Bn^2\sum_{m=-\infty}^{\infty} \mathrm{sgn}(ml)R_{ml}V_mV_l \quad (2)$$

where $l = n-m$, $A_n = \alpha_n x_0$ is an absorption parameter in terms of the small signal attenuation coefficient α_n at frequency $n\omega_0$, $B = x_0/\bar{x}$ is a dimensionless source amplitude expressed in terms of the distance $\bar{x}$ that characterizes the nominal shock formation distance for a plane wave, and R_{ml} is a matrix of coupling coefficients for the harmonic interactions. A model similar to Eq. (2), but without an absorption term, was proposed by Parker.[7]

Asymptotic quasilinear solutions of Eq. (2) for the farfield of the fundamental and second harmonic components have been derived for arbitrary amplitude distributions at the source. The results are similar (apart from decay rates) to those obtained for sound beams in fluids, and shall not be presented here. Instead, attention is focused on numerical solutions of the fully nonlinear system.

To integrate Eq. (2) numerically with the diffraction term included, it is convenient to introduce a coordinate system which follows the divergent spreading of the beam.[8] The appropriate transformation for a cylindrically spreading beam is defined as follows:[2,9]

$$\overline{V}_n(X,\overline{Y}) = V_n(X,Y)\sqrt{X+\delta}\exp\left(-\frac{inY^2}{X+\delta}\right) \qquad \overline{Y} = \frac{Y}{X+\delta} \quad (3)$$

where δ is a parameter that controls the divergence ($\delta > 0$) or convergence ($\delta < 0$) of the original coordinate system. Elimination of V_n and Y in Eq. (2), in favor of $\overline{V}_n$ and $\overline{Y}$, yields

$$\frac{\partial \overline{V}_n}{\partial X} + \frac{1}{4in(X+\delta)^2}\frac{\partial^2 \overline{V}_n}{\partial \overline{Y}^2} + A_n\overline{V}_n = -\frac{Bn^2}{\sqrt{X+\delta}}\sum_{m=-\infty}^{\infty} \mathrm{sgn}(ml)R_{ml}\overline{V}_m\overline{V}_l \quad (4)$$

The results presented below were obtained by solving Eq. (4) with finite difference methods (following minor modifications) that are commonly used to integrate the spectral form of the KZK equation.[10]

The results were calculated for a monofrequency source with a uniform rectangular amplitude distribution as a function of the transverse coordinate Y:

$$\begin{aligned} V_1(0,Y) &= 1 \qquad |Y| \le 1 \\ &= 0 \qquad |Y| > 1 \\ V_n(0,Y) &= 0 \qquad n > 1 \end{aligned} \tag{5}$$

This source condition is a common model for interdigital transducers that are used on surface acoustic wave devices.[4] Investigations based on other source conditions, including focused and asymmetric sources, are reported elsewhere.[2,9] The values $A_1 = 10^{-2}$ and $B = 1$ were used in all computations, and the attenuation coefficients depend quadratically on frequency ($A_n = n^2 A_1$). All numerical results presented below are for the free surface $Z = 0$, and they are based on a coefficient matrix R_{ml} that was evaluated with parameters for steel.[1,5]

Presented in Fig. 1 are (a) axial propagation curves and (b) beam patterns for the lowest four harmonic components in a Rayleigh wave beam of finite amplitude. The results are qualitatively similar to those for finite amplitude sound that is radiated into a viscous fluid by a uniform circular source.[8] In particular, efficient harmonic generation occurs mainly in the nearfield ($X < 1$), and the beam pattern for the nth harmonic component possesses n times as many sidelobes as are predicted by linear theory. The beam pattern for the fundamental component has a flatter main lobe and higher sidelobes than are predicted by linear theory (because of shock formation in the main lobe), which is again consistent with the results for finite amplitude sound in fluids.

Axial waveforms for the horizontal velocity component, at three distances from the source, are presented in Fig. 2. At $X = 1.5$, the sharpening of the peak and the

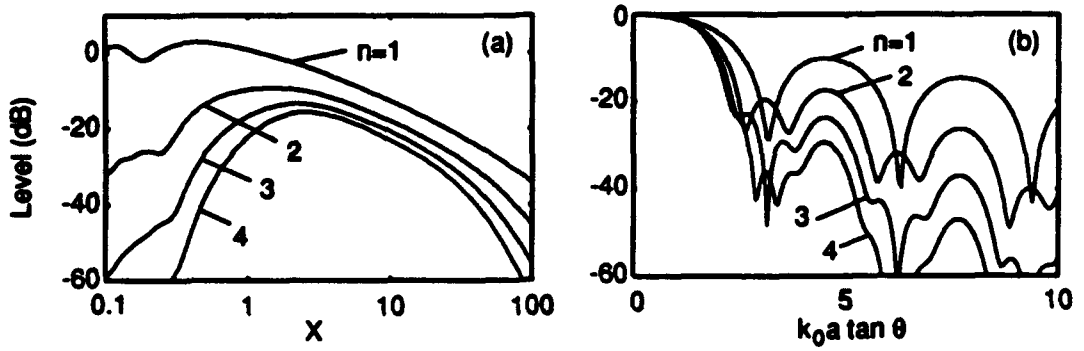

Figure 1: (a) Axial propagation curves ($Y = 0$) and (b) beam patterns at $X = 10$ for the lowest four harmonic components in a Rayleigh wave beam.

rounding of the trough are characteristic of the effect of diffraction on waveforms in fluids. However, the waveform asymmetry in a cylindrically spreading (two dimensional) beam is less than in a spherically spreading (three dimensional) beam. The waveform asymmetry in Fig. 2 is even less noticeable at $X = 3$, where a cusped sawtooth profile, similar to that predicted for plane waves, has formed. Note the approximately $\pi/4$ phase advance in the positions of the shocks, which agrees with linear diffraction theory for the phase of the fundamental component in the farfield.

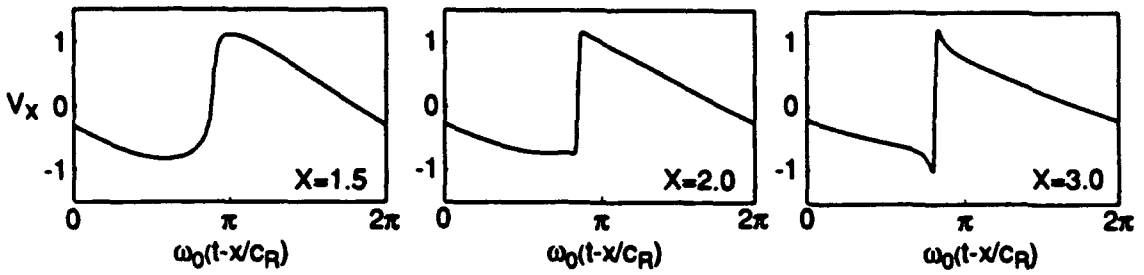

Figure 2: Horizontal velocity waveforms along the axis of a beam.

Finally, transverse amplitude distributions for the lowest three harmonic components in the nearfield of the beam, at $X = 0.18$ (which is the location of the last axial minimum in the nearfield of the fundamental component), are presented in Fig. 3. The distribution for the fundamental component is very close to that predicted by linear theory.[4]

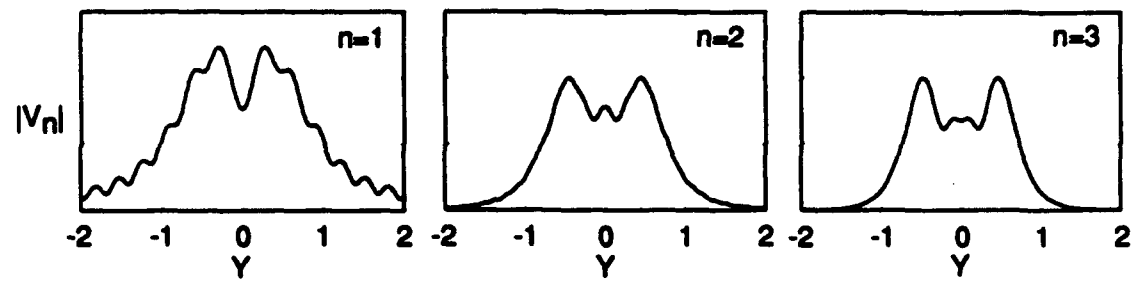

Figure 3: Transverse harmonic amplitude distributions in the nearfield of a beam ($X = 0.18$). A different vertical scale is used for each of the harmonics.

B. Local and Nonlocal Nonlinearity in Rayleigh Waves

Results from this work were presented[11] at the 125th Meeting of the Acoustical Society of America in Ottawa, Canada (May 1993). An article is currently in preparation for submission to *Journal of the Acoustical Society of America*.

Previous theoretical investigations of waveform distortion and shock formation in finite amplitude Rayleigh waves are based on periodic waveforms, mainly

waveforms that are sinusoidal at the source. Theoretical investigations of pulsed nonlinear Rayleigh waves, e.g., those which are exploited in nonlinear signal processing applications of surface acoustic wave (SAW) devices, are based on simple quasilinear models of the form[12]

$$v_3(t) = \iint_T h(t-t', t-t'') v_1(t') v_2(t'')\, dt'\, dt'' \tag{6}$$

Here $v_1(t)$ and $v_2(t)$ are signals whose weak nonlinear interaction produces a secondary signal $v_3(t)$ at a given location, $h(t_1, t_2)$ is an impulse response, and T is an interval that includes the duration of the interaction (or, alternatively, it is an integer number of periods in a time harmonic system). In models such as Eq. (6), $h(t_1, t_2)$ is simply a delta function that accounts for time delays associated with the interacting waves.

Several limitations of Eq. (6) can be noted. First, the theoretical model is quasilinear and can thus account only for weakly nonlinear effects, such as sum and difference frequency generation in harmonic waves, or products which can be associated with convolutions or correlations of the pulsed signals v_1 and v_2. It cannot account for the nonlinear distortion of a Rayleigh as it propagates, and it cannot account for shock formation. Second, the impulse response $h(t_1, t_2)$ is based on empirical results—no analytical expressions for $h(t_1, t_2)$ have appeared in the literature. Third, the assumption that $h(t_1, t_2)$ is proportional to delta functions is equivalent to the assumption that the nonlinearity in Rayleigh waves is entirely local. However, it is known that nonlinearity in Rayleigh waves is nonlocal, as pointed out first by Parker and Talbot.[13]

Zabolotskaya[1] showed that the evolution equation for the horizontal velocity component at the surface of an isotropic solid may be written in the form

$$\frac{\partial v}{\partial x} = \frac{C}{c_R^2 T^2} \frac{\partial}{\partial \tau} \iint_T L(\tau - \tau', \tau - \tau'') v(x, \tau') v(x, \tau'')\, d\tau'\, d\tau'' \tag{7}$$

where $v(x, \tau)$ is the horizontal velocity component, x is distance, $\tau = t - x/c_R$ is a retarded time, L is the kernal of the integral operator, and C is a dimensionless constant. In her original paper,[1] the kernel L was expressed as the Fourier series

$$L(t_1, t_2) = \sum_{m,l} |m + l| R_{ml} e^{-im\omega_0 t_1 - il\omega_0 t_2} \tag{8}$$

where R_{ml} is the same matrix that appears in Eq. (2).

During the past year, it was shown that L can be expressed in the explicit time-domain form

$$L(t_1, t_2) = T^2 \left[A\delta(t_1)\delta(t_2) + \frac{B(t_1/t_2)}{t_1^2 + t_2^2} \right] \tag{9}$$

where A is a dimensionless constant, B is dimensionless function of the ratio t_1/t_2, and δ is the Dirac delta function. Explicit expressions for A and B (as well as

C), in terms of second and third order elastic constants of the material, have been derived. Substitution of Eq. (9) in Eq. (7) yields

$$\frac{\partial v}{\partial x} = \frac{C}{c_R^2}\left[A\frac{\partial v^2}{\partial \tau} + \frac{\partial}{\partial \tau}\iint_T B\left(\frac{\tau - \tau'}{\tau - \tau''}\right)\frac{v(x,\tau')v(x,\tau'')\,d\tau' d\tau''}{(\tau - \tau')^2 + (\tau - \tau'')^2}\right] \qquad (10)$$

Setting $B = 0$ in Eq. (10) produces an equation identical in form to that for plane sound waves of finite amplitude in a lossless fluid. Nonlinearity in fluids is entirely local: finite amplitude distortion at an instant on the waveform is determined (in the preshock region) by the value of $\partial v^2/\partial \tau$ at that same instant. The first term on the right-hand side of Eq. (9) is thus associated with local nonlinear effects. In contrast, nonlinearity due to the integral in Eq. (10), at a given instant τ, depends on the value of v at all instants τ. The second term on the right-hand side of Eq. (9) is thus associated with nonlocal nonlinear effects. The nonlocal nonlinearity in Rayleigh waves is what distinguishes their finite amplitude properties from those of sound waves in fluids.

Comparison of Eqs. (6) and (10) illustrates the limitations of Eq. (6) that were discussed above. Equation (10) describes the evolution of the signal throughout its path of propagation, not just at a single point; it accounts for waveform distortion and shock formation; it is derived rigorously in terms of second and third order elastic constants of the material; and it accounts for nonlocal as well as local nonlinear effects.

Although Eq. (10) is an *explicit evolution* equation for nonlinear Rayleigh waves, and it provides substantial insight into the nature of the nonlinearity, its form is not the most convenient for performing numerical calculations (e.g., such as those required to describe waveform distortion, as depicted in Fig. 2). Instead, a differential evolution evolution which is currently under development [Eq. (4) of the previous annual summary report[14]] provides a more practical means of performing time domain calculations for nonlinear Rayleigh waves.

C. Pulsed Nonlinear Rayleigh Waves

The following results for pulsed Rayleigh waves were obtained by Knight, who entered the M.A. program in the Physics Department in fall 1992. Knight receives her salary support from Los Alamos National Laboratory.

As noted above, there are no reported theoretical predictions of nonlinear distortion and shock formation in pulsed Rayleigh waves. In fact, numerical simulations of even periodic Rayleigh waveforms, well beyond the point of shock formation, have been calculated only on the basis of Zabolotskaya's model equations.[1,3,5] There are presently three approaches that may be followed to investigate pulsed nonlinear Rayleigh waves numerically. One is to construct repeated sequences of pulses with harmonic series and then solve an equation similar to Eq. (2). Equation (7) can also be used, but the convolution is very time consuming. Finally, the differential

evolution equation which is discussed in the previous annual summary report[14] can be used (this work is currently in progress). Here, the first approach is used to obtain numerical results for plane wave pulses. Equation (2) is rewritten in terms of different dimensionless quantities:

$$\frac{\partial V_n}{\partial X} + A_n V_n = -\frac{n^2}{N} \sum_{m=-\infty}^{\infty} \mathrm{sgn}(ml) R_{ml} V_m V_l \tag{11}$$

where $X = x/\overline{x}$ and $A_n = \alpha_n \overline{x}$. The distance and attenuation parameters are now scaled according to $\overline{x}$, the nominal shock formation distance in steel at the center frequency of the pulse. The center frequency is taken to be the Nth harmonic in the Fourier series expansion. Waveforms are again obtained from Eqs. (1). Care must be taken that the repetition rate of the pulses described by the Fourier series is sufficiently low that successive pulses do not interact with each other.

Shown in Fig. 4 are predictions for the propagation of a short tone burst (center frequency ω_0) with a Gaussian envelope function, for $A_N = 0.01$. The center frequency of the source waveform, ω_0, is $N = 20$ times the fundamental frequency in the Fourier series representation. Replicas of the pulses shown in Fig. 4 are repeated at $\omega_0 \tau / 2\pi = 20n$, where $n = \pm 1, \pm 2, \ldots$. The number of harmonics retained in the computations was 500, which corresponds to 25 harmonics of the center frequency at the source.

The horizontal and vertical velocity waveforms are shown (as functions of distance X) in the second and third columns of Fig. 4, respectively. In the first column, for comparison, are predictions for the propagation of sound in a fluid (based on the Burgers equation), at distances where the distortion is similar to that in the horizontal component of the Rayleigh wave particle velocity. The ranges at which the calculations for fluids are compared with the calculations for Rayleigh waves are based on comparisons of the shock formation distances. Specifically, waveforms are compared at distances that are the same when normalized by the distance where shock formation first occurs in an initially sinusoidal wave at the center frequency of the source. The dimensionless absorption coefficients are also adjusted accordingly.

Comparison of the waveforms in the first two columns reveals that the propagation of a Rayleigh wave pulse resembles somewhat the propagation of an acoustic pulse in a fluid. One main distinction, as in the case of periodic waves,[1,5] is the cusping near shocks in the Rayleigh waves. In contrast, sound waves in fluids have more of a sawtooth profile (e.g., at $X = 10$). Beyond the shock wave region, both waveforms experience self-demodulation and tend toward a wave shape that is more closely related to the envelope of the source waveform than to the center frequency. Comparison of the waveforms at $X = 400$ and $X = 1200$ reveals that the absorption in this example is sufficiently weak that the demodulated waveforms are beginning to form shocks. Moreover, the "N wave" predicted in the fluid at

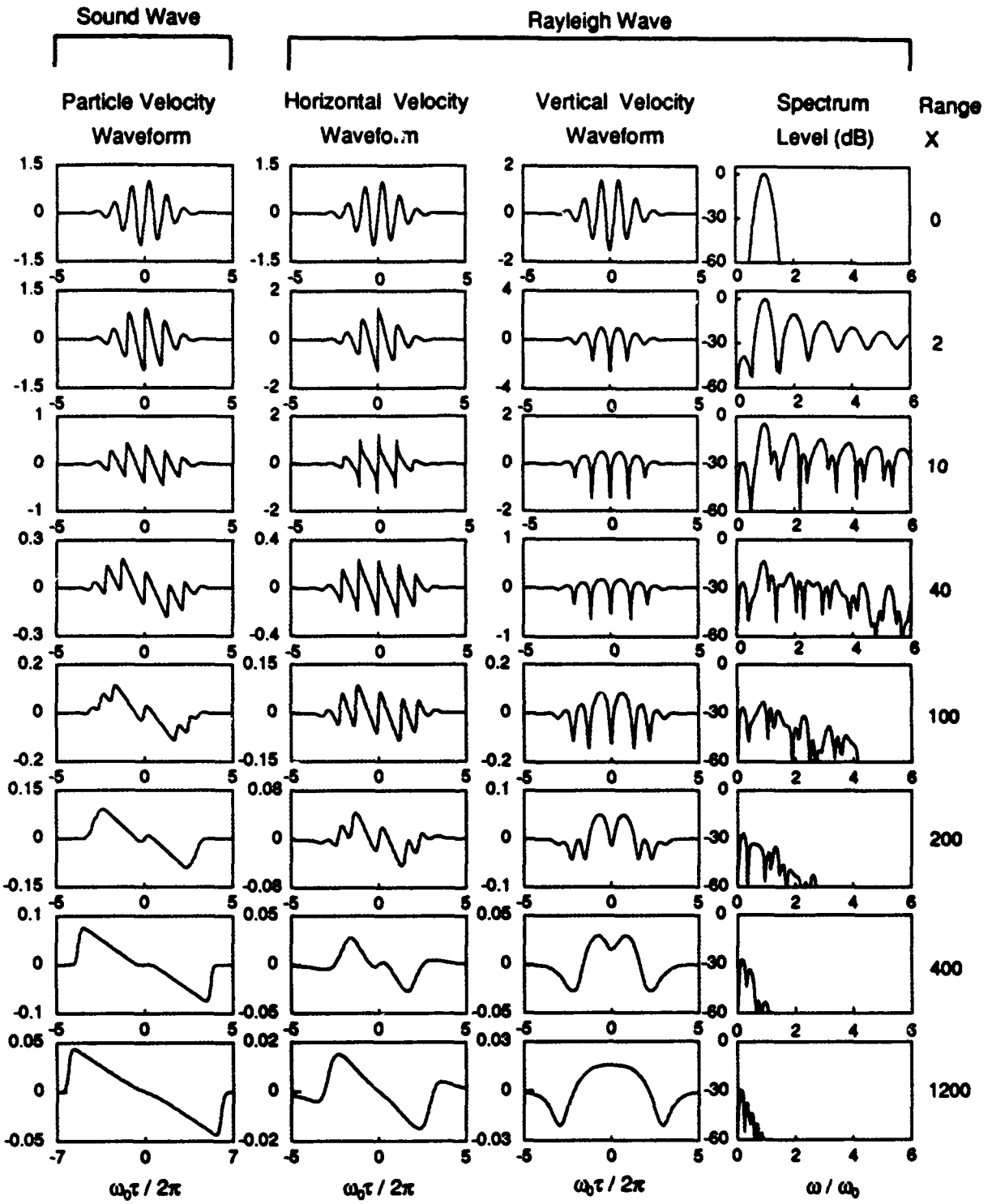

Figure 4: Horizontal velocity waveforms (second column), vertical velocity waveforms (third column), and corresponding frequency spectra (fourth column) for a nonlinear Rayleigh wave pulse, as functions of distance. In the first column are comparable results for sound waves in fluids..

$X = 1200$ has twice the amplitude of the horizontal component of the Rayleigh wave, and the head and tail shocks have already begun to move away from each other.

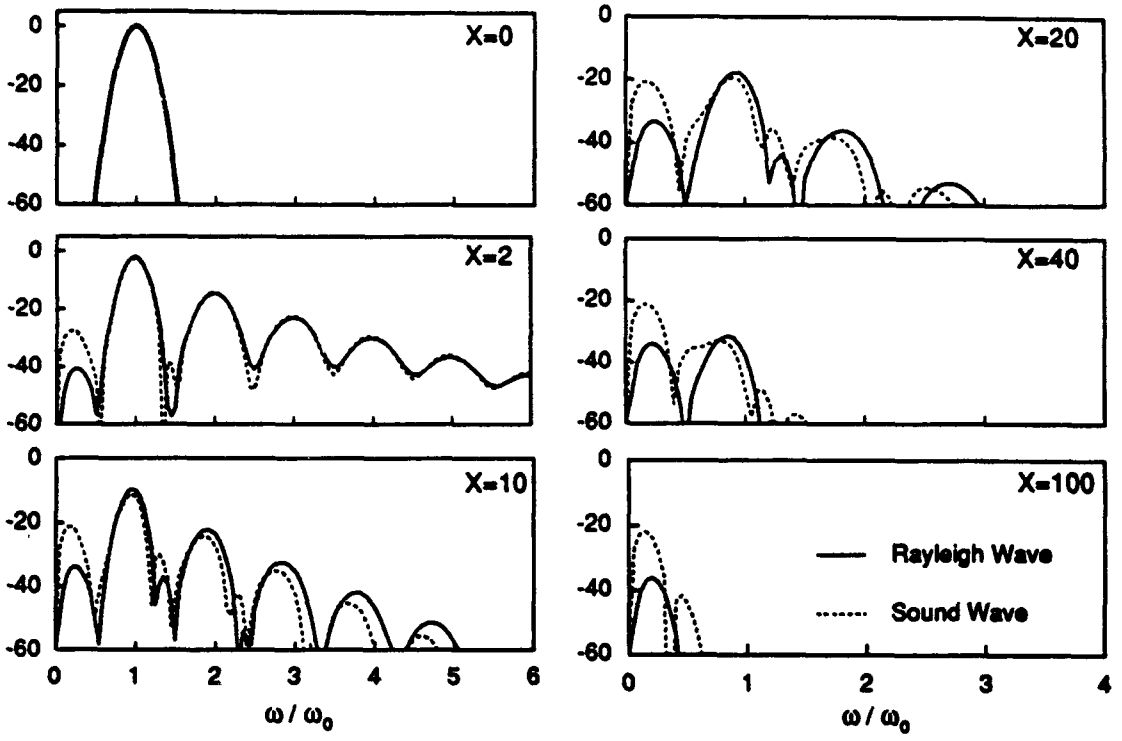

Figure 5: Comparison of frequency spectra for pulses similar to those in Fig. 4, but with higher attenuation..

In Fig. 5 are shown comparisons of frequency spectra for Rayleigh waves (solid lines) and for sound waves (dashed lines) in fluids, again at distances that are matched according to the scheme described above. Here, the absorption is ten times greater than in Fig. 4 ($A_N = 0.1$). At $X = 2$, the generation of higher harmonics in Rayleigh waves and sound waves is very similar, both in terms of spectral amplitudes and bandwidths. Note, however, that the generation of "difference frequencies" (i.e., spectral components below the frequency band of the primary wave) is more efficient in sound waves than in Rayleigh waves. [This effect can be demonstrated analytically by comparing quasilinear solutions, for sound waves and Rayleigh waves, for the case of sum and difference frequency generation.] The spectra in Fig. 5 thus assist interpretation of the waveforms in the first two columns of Fig. 4. Up to $X = 10$ in Fig. 4, the processes of distortion and shock formation, which are determined mainly by higher harmonic generation, are very similar in sound waves and Rayleigh waves. At $X = 40$, the stronger difference frequency generation in the fluid can be noticed. Comparison of the sound wave

at $X = 200$ and the Rayleigh wave at $X = 400$ reveals that the sound wave in this example demodulates in approximately half the distance required for the Rayleigh wave, and the final waveform in the fluid has nearly twice the amplitude as the Rayleigh wave.

D. Nonlinear Stoneley waves

This research is being performed by Meegan, who is supported by ONR through the AASERT program. Meegan entered the Ph.D. program in the Physics Department in fall 1992.

The main focus of Meegan's research is the development of a theoretical model for nonlinear Stoneley waves. The goal is to extend the model equation for Rayleigh waves, Eq. (11), to account for the spectral interactions in Stoneley waves. In principle, the method of accomplishing this task is straightforward. The Hamiltonian formalism employed by Zabolotskaya[1] to derive Eq. (11) for Rayleigh waves is easily adapted for application to Stoneley waves. The main difficulty is the amount of algebra required to derive the matrix R_{ml}, which is more cumbersome for Stoneley waves than for Rayleigh waves (even the algebra for Rayleigh waves is exceedingly tedious to accomplish by hand). The plan is to use the Mathematica symbolic computation software to overcome the obstacle presented by the algebra. The first step, the development a Mathematica program which reproduces Zabolotskaya's results for Rayleigh waves,[1] is completed. The relevant material parameters required to analyze nonlinear Stoneley waves have been identified, and therefore the remaining task is to modify the Mathematica program to calculate the nonlinearity matrix.

A second objective of Meegan's research is to obtain measurements of nonlinear Rayleigh waves that would complement recent theoretical predictions.[1,5] Our laboratory was not equipped previously to either generate or measure Rayleigh waves, and therefore time was devoted to development of the required facilities. Pinducer receivers have been purchased, and piezoelectric wedge transducers have been obtained for use as both sources and receivers. Preliminary measurements in aluminum have indicated the existence of harmonic generation due to finite amplitude propagation. However, poor signal-to-noise ratios are encountered even at the second harmonic frequencies, and therefore more efficient source and receiver configurations are being considered.

II. Pulsed Finite Amplitude Sound Beams

Portions of the work described in this section were performed by M. A. Averkiou and Y.-S. Lee. Lee successfully defended his Ph.D. dissertation in the Mechanical Engineering Department in July 1993. His dissertation describes the development of a computer code for solving the KZK equation for pulsed sound beams of finite amplitude in thermoviscous fluids. After he makes minor revisions in the dissertation, Lee will be eligible to graduate in December 1993.

A. Uniformly Valid Axial Solution for Self-Demodulation

This project, performed by Averkiou and Lee, is completed and is reported in two publications: in the Proceedings of the 13th International Symposium on Nonlinear Acoustics[15] (Bergen, Norway, June–July 1993); and in an article that is pending publication in *Journal of the Acoustical Society of America*.[16] The following discussion follows the former publication.[15]

Our investigation of the classic problem of self-demodulation was described in a previous annual report,[14] where comparison of experiment was made with numerical predictions.[17] In the process of completing that work, a simple yet very accurate analytic solution was developed for the field along the axis of the sound beam. The source is assumed to be a circular piston that vibrates with uniform amplitude in the plane $\sigma = 0$, i.e.,

$$\begin{aligned} P(0,\rho,\tau) &= f(\tau) \qquad \rho \le 1 \\ &= 0 \qquad\quad \rho > 1 \end{aligned} \tag{12}$$

where $P(\sigma,\rho,\tau)$ is a dimensionless pressure, σ is dimensionless range in terms of the Rayleigh distance, ρ is a dimensionless coordinate transverse to the axis of the beam, normalized by the piston radius, and τ is a dimensionless retarded time. The time dependence $f(\tau)$ is defined in terms of an amplitude modulation $E(\tau)$ and phase modulation $\phi(\tau)$ of a sinusoidal oscillation, as follows:

$$f(\tau) = E(\tau)\sin[\tau + \phi(\tau)] \tag{13}$$

The dimensionless expression for the instantaneous angular frequency is thus $\Omega(\tau) = 1 + d\phi/d\tau$. Now assume that $E(\tau)$ and $\phi(\tau)$ are slowly varying functions in comparison with $\sin\tau$. Combining various results of others,[18–21] we obtain for $A \gtrsim 1$ (absorption length less than the Rayleigh distance) and $\Gamma = \lesssim 1$ (where Γ is the Gol'dberg number), the following solution for the axial waveform:[16]

$$P(\sigma,0,\tau) = \left[f(\tau) - f(\tau-\sigma^{-1}) + \frac{\Gamma}{8\sigma}\frac{d^2}{d\tau^2}\left(\frac{E(\tau)}{1+d\phi/d\tau}\right)^2 \right] * \frac{\exp(-\tau^2/4A\sigma)}{\sqrt{4\pi A\sigma}} \tag{14}$$

where the asterisk indicates convolution with respect to τ.

The first two terms within the square brackets of Eq. (14) represent the center wave and edge wave, respectively, associated with the axial field of the primary beam radiated by a uniform piston source. The convolution of these two terms with the exponential dissipation function outside the brackets accounts for thermoviscous attenuation of the primary beam, which was investigated recently by Frøysa, Naze Tjøtta, and Tjøtta.[21] The third term in the square brackets is the farfield result for the low frequency, secondary pressure waveform produced by the distortion of the primary beam. With $\phi = \text{const}$, the third term reduces to the classical result of Berktay.[18] The factor $d\phi/d\tau$ accounts for the effect of phase modulation, which was considered by Gurbatov, Demin, and Malakhov.[19] Convolution of the third term with the dissipation function approximates the effect of thermoviscous attenuation on the secondary wave, in accordance with the approach followed by Cervenka and Alais.[20]

The accuracy of Eq. (14) can be tested against numerical results from the finite difference solution developed by Lee.[17] To perform this comparison we consider the limiting values $A = 1$ and $\Gamma = 1$ (agreement is expected to improve for larger A or smaller Γ). For the source waveform we let $E(\tau) = \exp[-(\tau/25\pi)^6]$ and $\phi(\tau) = -5\sin(\tau/25)$, which produces a pulse with sinusoidal frequency modulation. The dimensionless frequency of the carrier wave thus increases from $\Omega = 0.8$ in the center of the pulse to $\Omega \simeq 1.2$ at either end. In the left column of Fig. 6 is presented a comparison of time waveforms predicted by the finite difference solution (solid lines), and by Eq. (14) (dashed lines). In the right column of Fig. 6 are shown the corresponding frequency spectra S, normalized to yield peak amplitudes of unity at the source ($\sigma = 0$). The waveform and frequency spectrum at the source are presented in the top row, and the decibel values listed in each frame indicate the level relative to that at the source. Although they are not always easily distinguished, both dashed and solid lines are printed in each frame of Fig. 6.

Equation (14), despite the rather stringent conditions under which it was derived, is in good agreement with the numerical solution throughout the axial field. At $\sigma = 4$, the main effect that can be seen is due to thermoviscous dissipation of energy in the primary beam, which causes the ends of the pulse to attenuate more rapidly (because of the higher instantaneous frequency) than the middle. At $\sigma = 12$, the demodulated waveform dominates the contributions at the ends of the pulse, but the primary wave still dominates the middle. The final demodulated waveform is achieved at $\sigma = 24$. The positive pressures at the ends of the pulse are due primarily to amplitude modulation, and the negative pressure in the middle is due primarily to frequency modulation. Increasing A (with respect to the value of unity used in Fig. 6) leads to predictions by Eq. (14) which are virtually indistinguishable from the numerical predictions. Whereas the finite difference solution requires computation times on the order of ten minutes on a super computer, Eq. (14) requires only minutes on a personal computer.

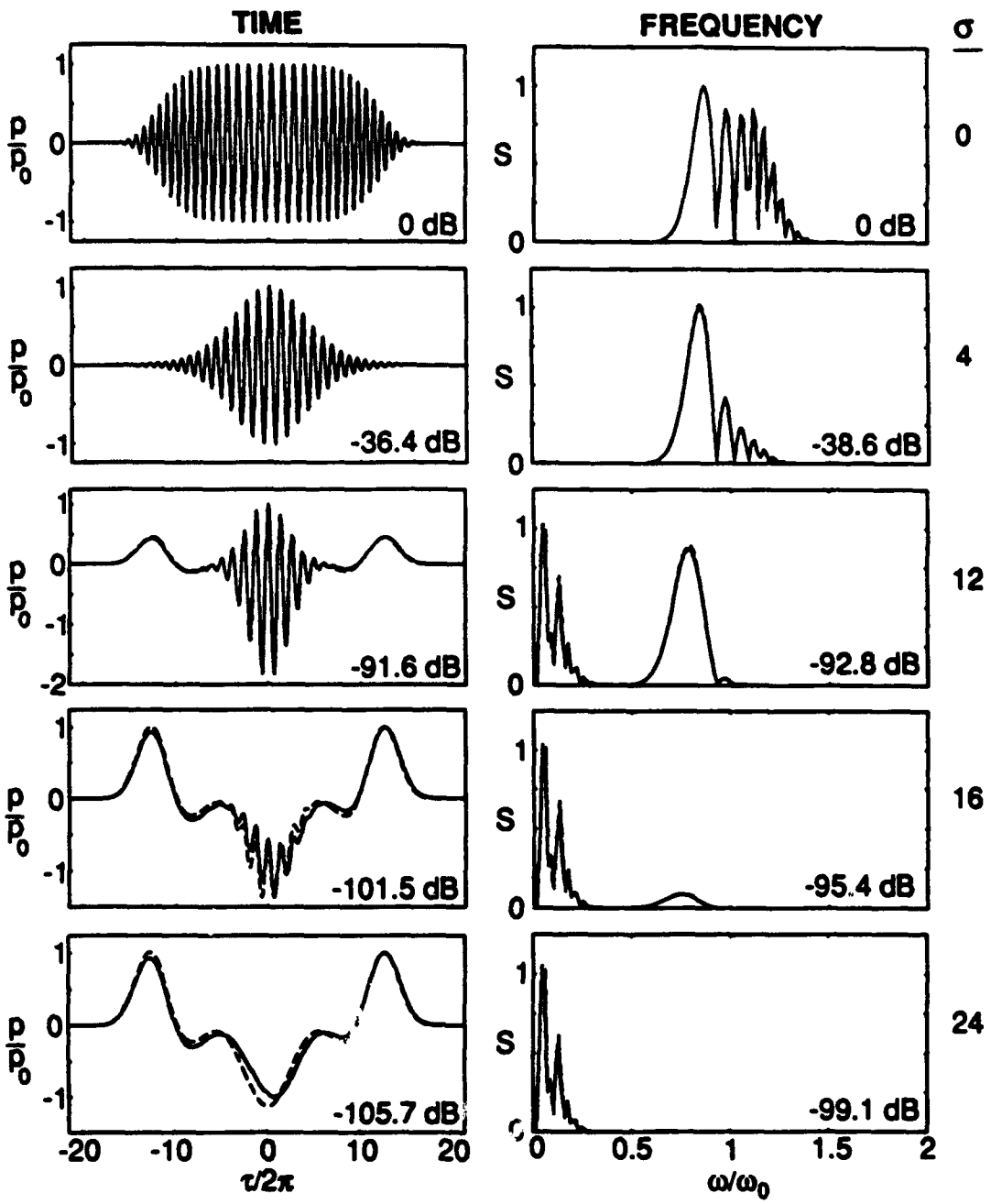

Figure 6: Left column: Comparison of the axial solution (dashed lines) with numerical results from the finite difference solution (solid lines) for a frequency modulated pulse ($\sigma = 0$), with $A = \Gamma = 1$. Right column: Frequency spectra of the waveforms in the left column (both dashed and solid lines).

B. Measurements of Pulsed Sound Beams in Water

This research was performed by Averkiou, and it will be reported at the fall 1993 meeting of the Acoustical Society of America in Denver. The following is the abstract that was submitted for that meeting:[22]

> Measurements are reported for finite amplitude acoustic pulses radiated by plane circular pistons in water. Pulses with center frequencies of several megahertz, peak sound pressures up to 1 MPa, durations ranging from approximately two to twenty cycles, and different amplitude and frequency modulations were investigated. Measurements of short pulses were made very near the source, where the center wave and edge wave can be separated. Pulse envelope distortion that accompanies shock formation in frequency modulated tone bursts is demonstrated. Acoustic saturation of pulsed sound beams is also investigated. All measurements are compared with theoretical predictions obtained from a computer code that solves the KZK equation in the time domain.[17] Very good agreement between theory and experiment is obtained both in the nearfield and the farfield, on and off axis. Artifacts in measurements of waveforms containing shocks, which are attributed to bandwidth limitations of membrane hydrophones, are discussed.

Representative samples of the results are shown in Fig. 7. The results are for radiation from a 1-inch diameter source in water at a center frequency of 1 MHz. The pulse envelope is Gaussian, and the equivalent shock formation distance for a plane wave is approximately twice the Rayleigh distance of the source. As before, $\sigma = z/z_0$ and $\rho = r/a$. The first three rows show axial waveforms beginning at the source ($\sigma = 0$) up to $\sigma = 2.9$, beyond the shock formation distance. The last three rows show waveforms across the beam at $\sigma = 2.9$, beginning on axis ($\rho = 0$) and moving out to $\rho = 5$. The frequency spectra in the last three rows reveal the increase in directivity as a function of increase in harmonic number. Agreement of theory and experiment, both on and off axis, is excellent.

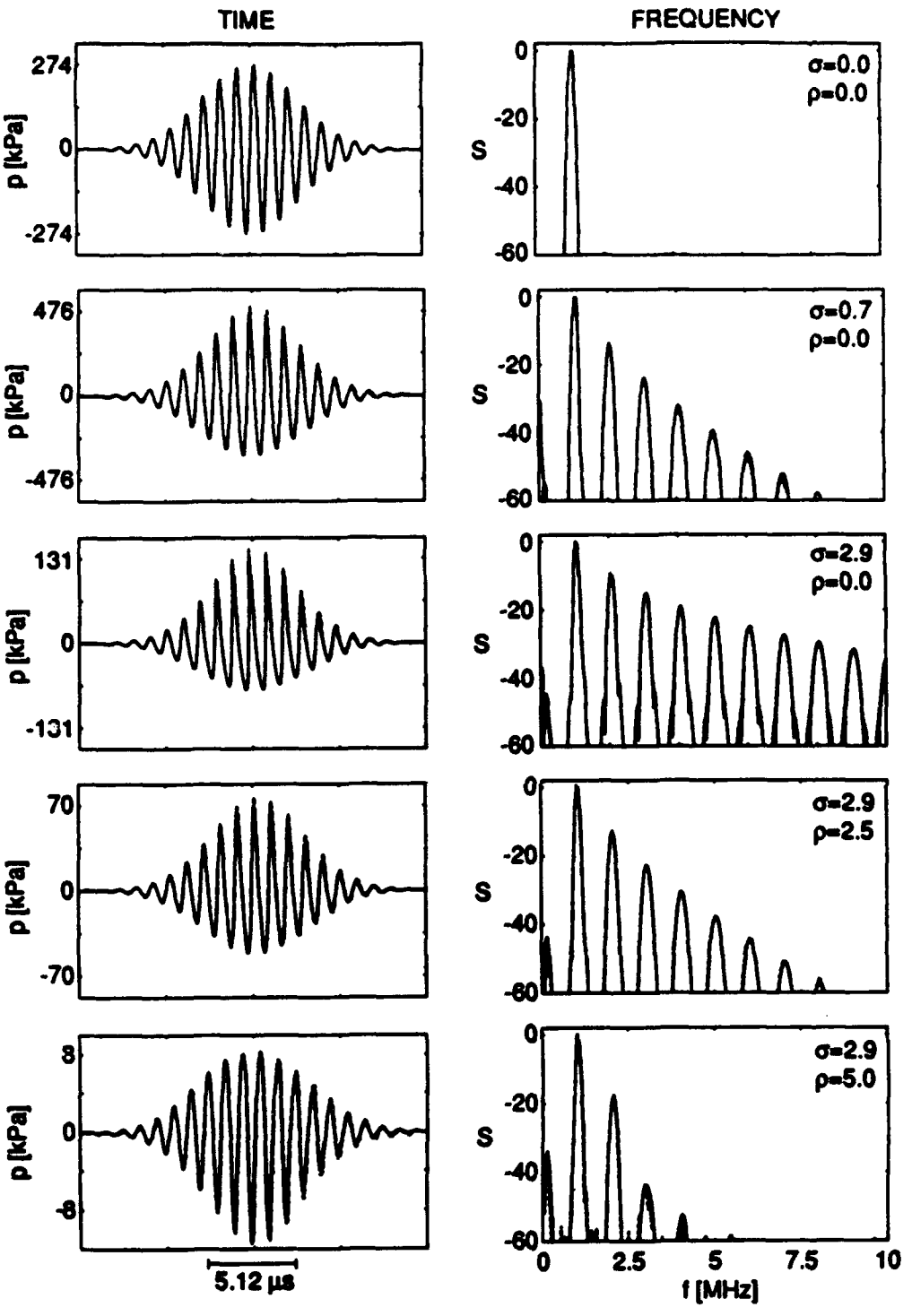

Figure 7: Waveforms and frequency spectra along the axis (from $\sigma = 0$ to $\sigma = 2.9$) and transverse to the axis (from $\rho = 0$ to $\rho = 5$) of a sound beam in water. The solid lines are calculated and the dashed lines are measured.

III. Finite Amplitude Sound in Waveguides

VanDoren completed his research on this project, and he received his Ph.D. in August 1993. The primary source of VanDoren's salary support during the past two years was a Rockwell Fellowship, and much of his equipment purchases were funded by the Packard Foundation. Here we report only the main results from his dissertation.

VanDoren considered the analysis of a waveguide formed by a horizontally stratified medium, with z designating the axis of the waveguide and x the transverse coordinate. Acoustic propagation in the waveguide is modeled by the following modified form of the Westervelt equation:

$$\frac{\partial^2 p}{\partial x^2} + \frac{\partial^2 p}{\partial z^2} - \frac{1}{c^2(x)} \frac{\partial^2 p}{\partial t^2} = -\frac{\beta}{\rho_0 c_0^4} \frac{\partial^2 p^2}{\partial t^2} \tag{15}$$

where p is the sound pressure, $c(x)$ accounts for weak variation of the sound speed transverse to the waveguide axis, and the right-hand side is the standard nonlinear term in the Westervelt equation. The procedure for solving Eq. (15) is an extension of the method outlined in Ref. 23. It is assumed that the solution may be expressed in the form

$$p = \frac{1}{2} \sum_m \sum_n p_{mn}(z) \phi_{mn}(x) e^{j(n\omega t - k_{mn} z)} + \text{c.c.} \tag{16}$$

where ϕ_{mn} are eigenfunctions that describe the transverse distributions of the normal modes (mode m, frequency $n\omega$) and satisfy boundary conditions at the walls (assumed parallel to the z axis), p_{mn} account for amplitude variations along the axis of the waveguide, and k_{mn} are axial wavenumbers obtained from linear theory. If the wall impedances are locally reactive, then the eigenfunctions are orthogonal, and the following approximate system of first-order equations can be obtained following substitution of Eq. (16) into Eq. (15):

$$p'_{mn}(z) + \alpha_{mn} p_{mn}(z) = \frac{j n^2 \omega^2 \beta}{4 k_{mn} \rho_0 c_0^4} \sum_r \sum_p \left[\sum_{q=1}^{\infty} g^{(1)}_{mnpqr}(z) + \sum_{q=1}^{n-1} g^{(2)}_{mnpqr}(z) \right] \tag{17}$$

where α_{mn} are attenuation coefficients that were introduced ad hoc, the function $g^{(1)}_{mnpqr}$ accounts for difference frequency generation, and $g^{(2)}_{mnpqr}$ accounts for sum frequency generation. The summations over r and p account for all combinations of modes in which the spectral components can interact, and the summation over q accounts for all frequency pairs that combine to yield the nth harmonic frequency component on the left-hand side. Equation (17) was solved with a standard fourth-order Runge-Kutta method.

A main advantage of the above solution technique is that the parabolic approximation is avoided, and accurate solutions are not restricted only to waves

that propagate at small grazing angles (with respect to the axis of the waveguide). In addition, the modal decomposition that is inherent in the solution facilitates physical interpretation of the results. An alternative and currently popular model equation for investigating finite amplitude sound in waveguides is the Nonlinear Parabolic Equation[24] (NPE). However, rather than make comparisons with solutions of the NPE, we compare results obtained from Eq. (17) with finite difference solutions of the KZK nonlinear parabolic equation, which is subject to the same general restrictions as NPE. The test case involved propagation in an air-filled rectangular duct with rigid walls (duct width of 6.6 cm in x direction) in which a primary wave at frequency 4350 Hz was excited in the lowest two modes. The two numerical solutions were compared with each other and with experiment.

Figure 8 shows the numerical solution of Eq. (17) (solid lines) compared with the numerical solution of the KZK equation (dotted lines) and experiment (circles) for the (a) primary wave and (b) nonlinearly generated second harmonic component due to a source level of 150 dB (re 20 μPa). Note that the solution of the KZK equation reveals phase errors, as a result of the parabolic approximation, at both $n = 1$ and $n = 2$, although the overall amplitudes are in good agreement with Eq. (17). Note the good agreement of Eq. (17) with the measurements.

Figure 9 shows comparisons of waveforms due to a source level of 154 dB. The high frequency oscillations in the first and third columns are Gibbs oscillations due to truncation of the Fourier series at 20 harmonics. Note the good agreement at all four ranges between Eq. (17) (first column) and experiment (second column). However, phase errors in the solution of the KZK equation manifest themselves as differences between the predicted and measured waveforms at $z = 2.11$ m and $z = 5.36$ m.

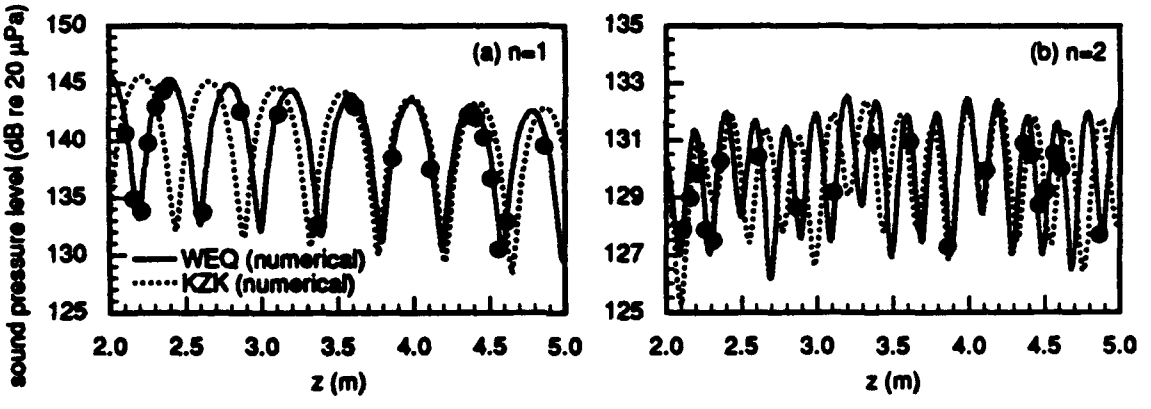

Figure 8: Propagation curves for (a) the primary wave and (b) the nonlinearly generated second harmonic component in a waveguide. Solid curves are obtained from Eq. (17), dotted curves from equations based on the parabolic approximation, and circles are measurements.

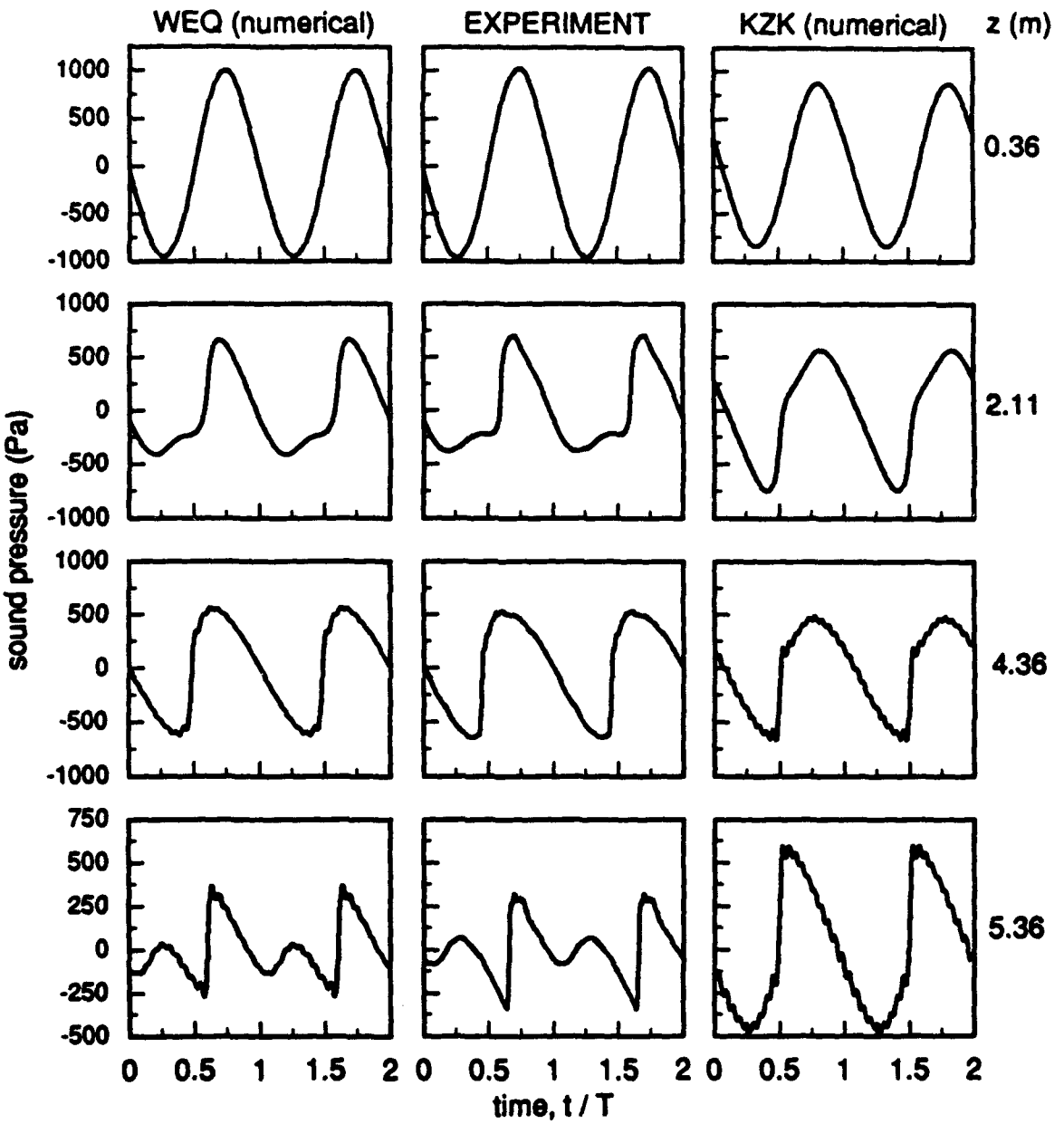

Figure 9: Calculated waveforms based on Eq. (17) (first column) and on the parabolic wave equation (third column). Measured waveforms are in the second column.

BIBLIOGRAPHY

[1] E. A. Zabolotskaya, "Nonlinear propagation of plane and circular Rayleigh waves in isotropic solids," *J. Acoust. Soc. Am.* **91**, 2569–2575 (1992).

[2] D. J. Shull, "Harmonic generation in plane, cylindrical, and diffracting nonlinear Rayleigh waves," M.S. Thesis, The University of Texas at Austin, May 1993.

[3] D. J. Shull, M. F. Hamilton, and E. A. Zabolotskaya "Nonlinear Rayleigh wave beams," *Advances in Nonlinear Acoustics*, edited by H. Hobæk (World Scientific, Singapore, 1993), pp. 496–501.

[4] T. L. Szabo, in *Physical Acoustics*, W. P. Mason and R. N. Thurston, eds., Vol. 13 (Academic Press, New York, 1977), Chap. 4.

[5] D. J. Shull, M. F. Hamilton, Yu. A. Il'insky, and E. A. Zabolotskaya, "Harmonic generation in plane and cylindrical nonlinear Rayleigh waves," *J. Acoust. Soc. Am.* **94**, 418–427 (1993).

[6] E. A. Zabolotskaya, "Nonlinear Rayleigh waves in an isotropic solid," *Proceedings of the 14th Scandinavian Cooperation Meeting in Acoustics/Hydrodynamics*, edited by H. Hobæk, Sci./Tech. Rep. No. 1991-09, Deptartment of Physics, University of Bergen, Norway (1991), pp. 65–78.

[7] D. F. Parker, "Nonlinear surface acoustic waves on homogeneous media," in *Nonlinear Waves in Solid State Physics*, edited by A. D. Boardman, M. Bertolotti, and T. Twardowski (Plenum Press, New York, 1990), pp. 163–193.

[8] M. F. Hamilton, J. Naze Tjøtta, and S. Tjøtta, "Nonlinear effects in the farfield of a directive sound source," *J. Acoust. Soc. Am.* **78**, 202–216 (1985).

[9] E. E. Kim, "Nonlinear effects in asymmetric cylindrical sound beams," M.S. Thesis, The University of Texas at Austin, December 1990.

[10] J. Berntsen and E. Vefring, "Numerical computation of a finite amplitude sound beam," Rep. No. 81, Department of Applied Mathematics, University of Bergen, Norway (1986).

[11] M. F. Hamilton, Yu. A. Il'insky, and E. A. Zabolotskaya, "Rayleigh wave nonlinearity," *J. Acoust. Soc. Am.* **93**, 2384 (1993).

[12] M. Feldmann and J. Hénaff, *Surface Acoustic Waves for Signal Processing* (Artech House, Boston, 1989), Chap. 7.

[13] D. F. Parker and T. M. Talbot, "Analysis and computation for nonlinear elastic surface waves of permanent form," *J. Elast.* **15**, 389–426 (1985).

[14] M. F. Hamilton, "Problems in nonlinear acoustics," Fourth Annual Summary Report under ONR Grant N00014-89-J-1003, Department of Mechanical Engineering, The University of Texas at Austin, August 1992.

[15] M. A. Averkiou, Y.-S. Lee, and M. F. Hamilton, "Self-demodulation revisited," *Advances in Nonlinear Acoustics*, edited by H. Hobæk (World Scientific, Singapore, 1993), pp. 251–256.

[16] M. A. Averkiou, Y.-S. Lee, and M. F. Hamilton, "Self-demodulation of amplitude and frequency modulated pulses in a thermoviscous fluid," *J. Acoust. Soc. Am.* (in press).

[17] Y.-S. Lee and M. F. Hamilton, "Nonlinear effects in pulsed sound beams," *Ultrasonics International 91 Conference Proceedings* (Butterworth-Heinemann, Oxford, 1991), pp. 177–180.

[18] H. O. Berktay, "Possible exploitation of non-linear acoustics in underwater transmitting applications," *J. Sound Vib.* **2**, 435–461 (1965).

[19] S. N. Gurbatov, I. Yu. Demin, and A. N. Malakhov, "Influence of phase fluctuations on the characteristics of parametric arrays," *Sov. Phys. Acoust.* **26**, 217–220 (1980).

[20] P. Cervenka and P. Alais, "Fourier formalism for describing nonlinear self-demodulation of a primary narrow ultrasonic beam," *J. Acoust. Soc. Am.* **88**, 473–481 (1990).

[21] K.-E. Frøysa, J. Naze Tjøtta, and S. Tjøtta, "Linear propagation of a pulsed sound beam from a plane or focusing source," *J. Acoust. Soc. Am.* **93**, 80–92 (1993).

[22] M. A. Averkiou and M. F. Hamilton, "Measurements of finite amplitude pulses radiated by plane circular pistons in water," abstract to appear in *J. Acoust. Soc. Am.* **94** (1993).

[23] M. F. Hamilton and E. A. Zabolotskaya, "Dispersion," in *Nonlinear Acoustics*, edited by D. T. Blackstock and M. F. Hamilton (Academic Press, New York, in preparation).

[24] J. J. Ambrosiano, D. R. Plante, B. E. McDonald, and W. A. Kuperman, "Nonlinear propagation in an ocean acoustic waveguide," *J. Acoust. Soc. Am.* **87**, 1473–1481 (1990).